GSMMC19: Cutting with Water

Lauren Barnes[1], Katelynn Huneycutt[2], Elita Lobo[3], Nick Mazzoleni[4], Jenna McDanold[5], Richard Moore[1], Aprajita Singh[6], Jerome Troy[7], and Thomas Tu[8]

[1]New Jersey Institute of Technology
[2]University of Maryland, Baltimore County
[3]University of Massachusetts, Amherst
[4]North Carolina State University
[5]Rochester Institute of Technology
[6]University of Texas, Dallas
[7]University of Delaware
[8]University of California, Los Angeles

June 15, 2019

1 Introduction

At MPI 2013, OMAX, a waterjet cutting machine manufacturing company, presented several interesting modeling problems. The ones which we focused on were striations left on materials after being cut, residue after finishing a cut, and the oscillation in the stream.

Cutting technologies such as waterjets, lasers, or plasma often leave undesired wavy rough trace marks as a byproduct on the surface of the material being cut. These wavy marks are called striations. The abrasive waterjet generally results in an upper smooth zone and a lower rough zone characterized by arc-like striations in the direction orthogonal to the traverse. Minimizing the surface striations and hence getting a smooth cut is one of the main unresolved challenges in waterjet cutting.

Several attempts have been made to explain the cause of the striation phenomena; however, very few have been able to derive mathematical models that estimate the relation between various configuration parameters like velocity of jet stream, traverse velocity, jet stream diameter, type of abrasive material etc and the striation angle.

Hashish [6] conducted a visual investigation of AWJ cutting process using high speed photography and came to a conclusion that striations are a characteristic feature of the AWJ cutting process. He found that in the upper smooth

zone, material was removed by the impact of abrasive particles at shallow angles whereas in the lower rough zone,the material removal process was unsteady and led to large particle impact angles and formation of undulations on the walls of the cut surface.

In a study conducted by Chen et al [4], it was proposed that striations are formed mainly due to variation in the distribution of abrasive particle kinetic energy with respect to the cut surface. According to the authors, internal factors like the distribution of abrasive particles along the jet cross section result in a non-uniform distribution of particle kinetic energy. Since, in the upper zone most particles have sufficient kinetic energy to cut or erode the material, the cut surface is almost free of striation. As the particles penetrate the material, the number of particles that have kinetic energy above the necessary threshold value required for cutting the material decreases and these weak particles follow the traces of the other particles with high energy. This leaves wavy and rough trace marks on the surface. The authors also suggest that fluctuation or unsteadiness of the process parameters such as jet traverse speed, abrasive flow rate, water pressure and vibration in the cutting system could affect the distribution of kinetic energy of abrasive particles and contribute to striation formation. Additionally, they deduced that the striation drag angle depends on the ratio of the jet traverse speed in the horizontal direction to the jet vertical penetration rate.

In another model proposed by Raju and Ramulu, [8] it was demonstrated that the jet indeed oscillates in the plane normal to the cutting plane. Arola and Ramulu [2] proposed a striation formation model which aligns with the results from Chen's study and which showed that a jet with lower energy tends to deflect in the direction normal to the plane of cutting, which will result in striations forming on the cut surface if the jet energy is below the material cutting threshold.

Chao and Geskin [7] used spectral analysis to find the correlation between cut surface striation and machine vibrations, which they concluded was the primary cause of striations. The authors explained that the amplitude of vibration in the direction normal to the plane of cut increases as the depth of cut increases, which results in an increase in lateral oscillation and an increase in amplitude of cut surface striation. It was thus deduced that a reduction in the vibrations associated with the machine could effectively decrease the striations on the cut surface. They also found that the direction of cutting or jet traverse significantly affects the striation frequency and amplitude, and experimentally established that as the ratio between the traverse speed and jet penetration rate increases, the drag angle becomes larger.

In another study by Hashish [5], high-pressure abrasive waterjet cutting is viewed as an erosion process which is highly dependent on whether the eroded material is brittle or ductile in nature. The authors modify the existing erosion model by Finnie [3] to include the crater width variation as the depth of the trajectory varies. The new erosion model proposed introduces a jet velocity exponent of 2.5 and includes the particle shape, expressed by its sphericity and roundness.

Based on this erosion model, the authors further developed a model for predicting the depth of cut of abrasive waterjets in different metals. The erosion model is used with a kinematic jet-solid penetration model developed from visualization of cutting process to obtain expressions for depths of cut for varying modes of erosion along the cutting kerf.

In our study, we use Finnie's erosion model [3] and Hashish's striation prediction model [5] to study:

1. Variation in wear rate with K for Finnie's and Hashish's model where K is defined as the ratio of normal force to shear force applied to the cut surface. This shows how the wear rate is affected by traverse velocity and jet velocity.

2. Dependence of wear rate ($\frac{d(\text{depth of cut})}{dt}$) as a function of thickness measure of the material η for Hashish's and Finnie's model where η is defined as $H\frac{C_f}{d_j}$, C_f is the coefficient of friction of the abrasive material, d_j is the diameter of waterjet and H is the total depth of the material. This demonstrates how impact angle affects how the water jet erodes the material.

3. Variation in amplitude of oscillation with depth of cut and traversed distance.

We also derive a model using Finnie's erosion model to explain oscillation patterns in the waterjet as it penetrates the material.

1.1 OMAX Waterjet Specifications

The OMAX waterjets use material erosion by spraying a collimated stream of water and injecting some abrasive particle, typically garnet, into the material. Using the Bernoulli equation, we can calculate the outflow velocity of the water jet. Taking the initial pressure $P_1 \approx 6 \times 10^4$ psi, the final pressure $P_2 \approx 0$ (i.e., atmospheric), the density of the water $\rho \approx 10^3$ kg/m^3, and the initial velocity $v_1 = 0$, we can find the final velocity v_2, since

$$P_1 = \frac{1}{2}\rho v_2^2$$
$$\implies v_2 = \sqrt{2\frac{P_1}{\rho}} \approx 894 \text{ m/s}$$

We can also calculate the the fluid mass flow rate $\dot{M}_w$ using the fact that the diameter of the jet's nozzle $d_j = .7$mm

$$\dot{M}_w = \rho A v = 0.344 \text{ kg/s} \tag{1}$$

The garnet is injected into the stream with mass flow rate $\dot{M}_g \approx .01$ kg/s. Since the mass flow rate of fluid is 34 times that of the garnet, the effect of solute injection on the velocity is negligible.

Physical Parameter	Symbol	Approximate Values
Nozzle Diameter	d_j	$0.25 - 7$ mm
Pressure	P_1	$6.0\text{x}10^5 - 9.0\text{x}10^5$ psi
Abrasive Mass Flow Rate	$\dot{M}_g$	0.1 kg/s
Height of Material	H	20-30 mm
Traverse Velocity	v_T	1.4 mm/s
Density of Abrasive	ρ_p	3850 kg/m^3
Density of Material (Aluminum)	ρ_m	2700 kg/m^3
Amplitude of Striations	a_{max}	100-200 μm
Coefficient of Drag Friction of Material	C_f	0.001
Mass of Abrasive Particle	m	1-64 ng
Ratio of Contact Depth to Cut Depth	ψ	2
Ratio of Vertical to Horizontal Jet Forces	K	1.5-2.5
Flow Stress of Eroded Material	p	1000 MPa

Table 1: Physical Parameters

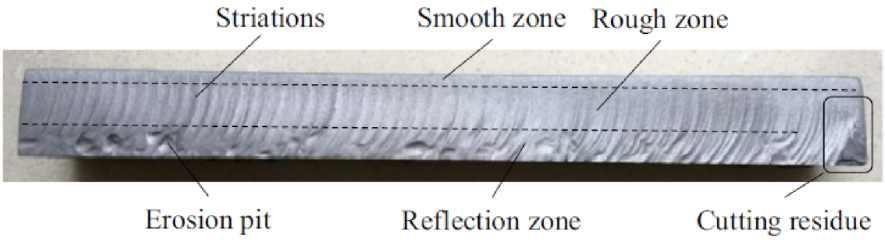

Figure 1: Issues arrising in using waterjet cutting techniques [1]

2 Striations

A number of physics-based models for waterjet cutters exist in the current literature. Both Finnie [3] and Hashish [6] have developed models for volume removed from the cutting surface. The generic form of the equation for volume removed is given by:

$$\dot{\tilde{V}}_m = \frac{\pi}{4} d_j^2 \dot{\tilde{z}} \tag{2}$$

where $\dot{\tilde{z}}$ is the time rate of waterjet penetration into the cutting surface. This rate of change is given by Finnie as:

$$\dot{\tilde{z}}^{(F)} = \frac{4 m_p \tilde{v_s^2}}{\pi d_j^2 \psi K} f(\alpha) \tag{3}$$

where m_p is the mass of abrasive particles in kg, v_s is the averaged velocity of the stream and abrasive particles in m/s, ψ is the ratio of contact depth to cut depth, K is the ratio of vertical to horizontal forces imparted by the jet on

the cutting surface, α is the angle of the jet stream with respect to the normal to the surface in radians in the direction of traversal (also called the angle of attack), and $f(\alpha)$ is functional dependence of the wear on the jet stream angle, given by

$$f(\alpha) = \begin{cases} \sin(2\alpha) - \dfrac{6\sin^2(\alpha)}{K}, & \text{when } \tan(\alpha) \leq \dfrac{K}{6} \\ \dfrac{K}{6}\cos^2(\alpha) & \text{when } \tan(\alpha) \geq \dfrac{K}{6} \end{cases} \tag{4}$$

This wear function is continuous and differentiable on $\left[0, \frac{\pi}{2}\right]$. Another model for the rate of penetration was developed by Hashish et al [6]. From this model, the rate of change of the depth $\dot{\bar{z}}^{(H)}$ is given by

$$\dot{\bar{z}}^{(H)} = \frac{28 m_p v_s^{5/2}}{\pi^2 d_j^2 \rho_p C_f^{5/2}} g(\alpha) \tag{5}$$

Where

$$g(\alpha) = \sin(2\alpha)\sqrt{\sin\alpha} \tag{6}$$

These models can predict things such as cutting depth and volume of material removed, but they make little attempt to predict the shape of the striation curve itself. We look to build a simple erosion model that accounts for the shape of the striation curves as a function of depth and cutting velocity.

2.1 Velocity as a Function of Depth

As the waterjet cuts into the material, the cutting velocity of the jet decreases as energy is lost due to friction. In Hashish's paper, the jet cutting velocity is calculated as a function of depth, considering the frictional drag from the wall of the material being removed. Hashish derived this velocity-depth relationship in [6] starting with the conservation of momentum:

$$\dot{m}_t v = \dot{m}_t v_0 - F_f \tag{7}$$

where $\dot{m}_t$ is the total mass flow rate of the water and abrasive particles, v is the velocity, v_0 is the initial velocity, and F_f is the drag friction force

$$F_f = \frac{\pi}{4} C_f d_j H \rho v_0^2 \tag{8}$$

where C_f is the coefficient of friction of the material.

Dividing by the mass flow rate yields

$$v = v_0 - \frac{\pi C_f}{4\dot{m}_t} d_j H \rho v_0^2. \tag{9}$$

For simplification purposes, combine the constants into one

$$K_w = \frac{\pi C_f}{4\dot{m}_t} d_j H \rho v_0, \tag{10}$$

and the equation for v becomes

$$v = v_0 - K_w H v_0 \tag{11}$$

We know $\dot{m}_t = \rho A v = \dfrac{\pi d_j^2 \rho v_0}{4}$, so K_w simplifies to be

$$K_w = \frac{C_f}{d_j} \tag{12}$$

Thus, we have that

$$\tilde{v}_s(z) = v_0 \left(1 - \frac{C_f}{d_j} z\right) \tag{13}$$

2.2 Nondimensionalization of Variables

We nondimensionalize our relevant variables from the previous analyses and rewrite our equations.

$$\tilde{h} = Hh \tag{14}$$

$$\tilde{z} = Hz \tag{15}$$

$$\tilde{t} = t/\omega \tag{16}$$

$$\eta = \frac{HC_f}{d_j} \tag{17}$$

$$\tilde{v}_s = v_0 v_s \tag{18}$$

In these equations, variables denoted with tildes are variables with dimensions, while t, v_s, and z are the dimensionless forms of the time, the velocity of the waterjet stream and abrasive particles into the material, and the penetration depth of the waterjet stream into the material, respectively. The nondimensional parameter η represents the maximum depth to which the material can be cut (which must be much less than unity). We can plug these nondimensionalized variables into Equations (3), (5), (13) to obtain:

$$\dot{z}^{(F)} = \frac{4mv_0^2}{4\pi d_j^2 K H \omega} v_s^2 f(\alpha) \tag{19}$$

$$\dot{z}^{(H)} = \frac{28mv_0^{5/2}}{\pi^2 d_j^2 \rho_p C_f^{5/2} H \omega} v_s^{5/2} g(\alpha) \tag{20}$$

$$v_s(z) = (1 - \eta z) \tag{21}$$

Equations (19) and (20) can be simplified by defining wear coefficients:

$$w_c^{(F)} = \frac{4mv_0^2}{4\pi d_j^2 K H \omega} \tag{22}$$

$$w_c^{(H)} = \frac{28 m v_0^{5/2}}{\pi^2 d_j^2 \rho_p C_f^{5/2} H \omega} \tag{23}$$

Rewriting, we have:

$$\dot{z}^{(F)} = w_c^{(F)} v_s^2 f(\alpha) \tag{24}$$

$$\dot{z}^{(H)} = w_c^{(H)} v_s^{5/2} g(\alpha) \tag{25}$$

2.3 Comparison of Models

In the plots below, we consider starting with an initial profile of the material and blasting it from the top with the jet beam in such a way that the center of the jet beam corresponds with the center of the profile as pictured in Figure 2.

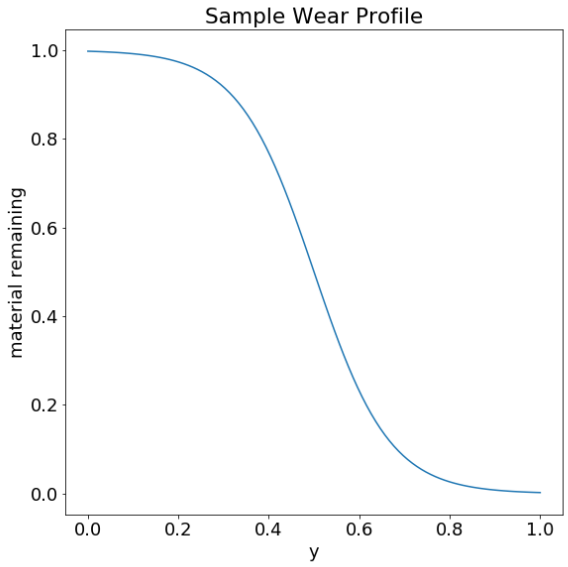

Figure 2: A sample profile of the material before the waterjet is turned on used to test the relations between wear, material height, and angle of attack.

After the waterjet is turned on, the resulting wear on the material in a given location on the material profile depends, according to the Finnie and Hashish models, on the parameter η. Recall from Equation (17) that η is proportional to H, the height (depth) of the material that is being cut.

Figure 3 compares the dependence of the wear rates of the profile on η, as predicted by the Hashish (Eq. 20) and Finnie models (Eq. 19). Note how the two models predict similar results: where there is greater curvature, there is

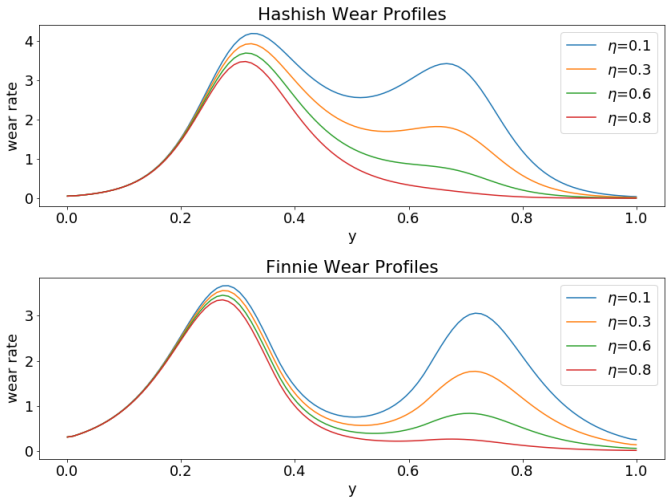

Figure 3: Plots of the wear rate for various values of η, as predicted by the Hashish (top panel) and Finnie (bottom panel) models.

more wear, and at the ends of the profile where it is fairly flat, there is less wear. As η is increased, we see from the plots below that the wear becomes more and more localized near the region on the left-hand side where the profile begins to curve steeply near the top.

As shown in Eq. (19), Finnie's model for material erosion depends on the ratio K of normal force to shear force. Figure 5 is a plot showing the dependence of the erosion (wear) rate on K, according to the Finnie model. Note that we again begin with the same initial material profile as in the plots above. Notice that, as K is increased, the localization of the wear at regions of greater curvature becomes more pronounced.

3 Steady State Profile

We used the Finnie and Hashish models in a simulation of a material being passed under a waterjet. We ran these simulations until the cut profile of the material reached steady state. To initiate these simulations, we assumed the material had a profile of hyperbolic tangent. We then simulated pushing this material under the waterjet stream and observed the wear profile evolution.

The resulting steady state profiles capture a slight nonlinearity in the shape of the striations. This seems to be caused by the jet losing cutting power as it penetrates further into the material being cut, as calculated by Hashish's velocity function. These results were obtained for the Finnie model of cutting, however the Hashish cutting model yielded numerical instabilities within the solution making capturing the steady state impossible.

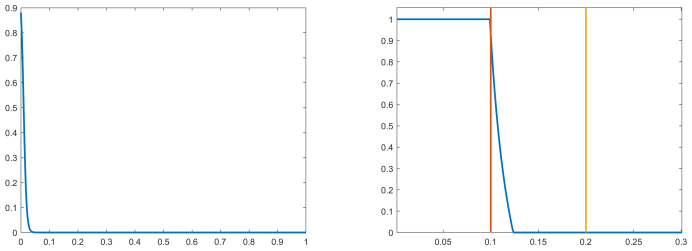

(a) Initial wear profile used in cutting simulations

(b) Steady state wear profile yielded by cutting simulations

Figure 4: Initial and steady state profiles of materials from cutting simulations. The red and yellow lines on the right figure indicate the start and stop of the waterjet steam respectively. Note only the Finnie model was used in simulations.

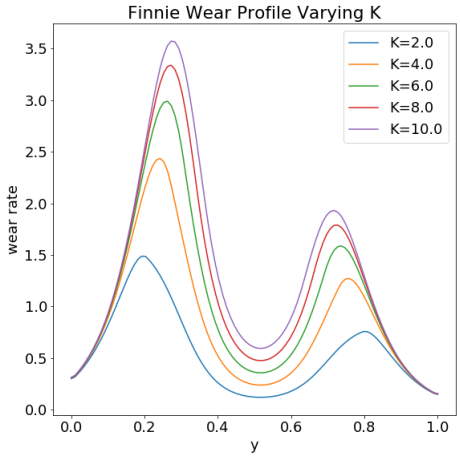

Figure 5: The wear rate of the initial profile given in 2, plotted for various values of K.

3.1 Steady State Profile Assuming Constant Wear Rate

Taking Finnie's model for ductile erosion[3], we find the steady state profile by assuming that the wear rate must be independent of height; otherwise, as the cut progresses, the profile would continue to change. Assuming velocity decreases with depth as in Hashish's model Equation (13), the angle of attack, α, must change to compensate. Thus, we have

$$\frac{dV_m}{dt} = \frac{\dot{M}_g v_s^2}{K\Psi p} f(\alpha) = \frac{v_T d(z) H}{\cos(\alpha)}$$

$$v_s = v_0 \left(1 - \frac{C_f}{d_j} z\right)$$

$$d(z) = d_j \sqrt{\frac{v_0}{v_s}}$$

where $\frac{v_T d_j H}{\cos(\alpha)}$ is the volume outflow rate due to traversal (adjusted for attack angle) and $d(z)$ is the diameter of the jet at height z assuming constant flux. We can then solve numerically for α in terms of z.

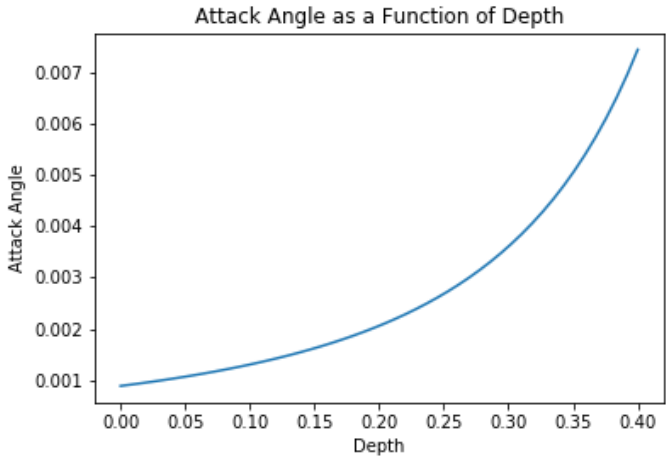

Figure 6: Attack angle α as a function of cut depth.

Since $\frac{dy}{dz} = \tan(\alpha)$, we can then numerically integrate for y, the displacement in the direction of traversal as a function of z, the cut depth.

4 Jet Oscillations

When the jet enters the material, the column moves in a straight line until some critical distance inside when it begins to oscillate in the perpendicular direction

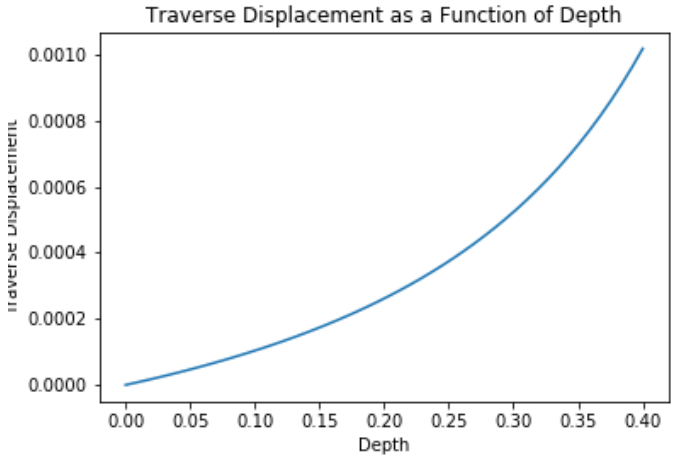

Figure 7: Residue width as a function of cut depth.

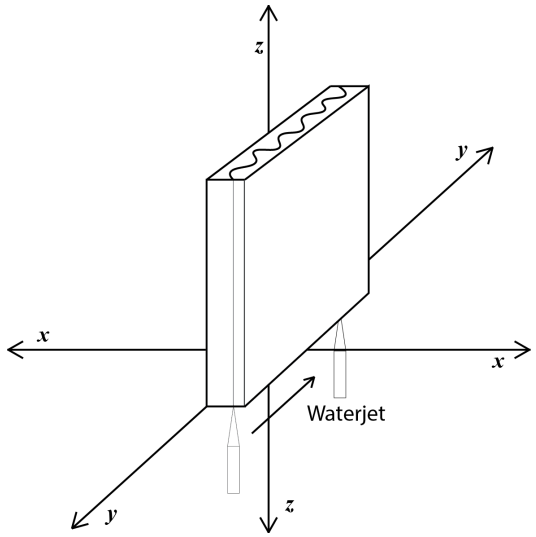

Figure 8: The water jet goes straight in one side of the material, but it oscillates as traverses the materaial.

to the direction of traversal. The amplitude of these oscillations then grows the deeper it is into the material. The result is a flopping of the water as it comes out of the base of the material and interesting oscillation patterns in the traverse direction throughout the material, but most defined on the bottom. While an initial displacement of the jet in one direction can be justified by a loss of energy as the jet bores into the material, the oscillations of the jet from one side to

another has no obvious physical explanation. Without such an explanation, we will use a simple model merely to match the shapes of the oscillations.
We know that as the jet gets deeper in the material the oscillations have greater amplitude. Using this, we can model the final area that has been carved out of the material as a decaying sine function:

$$\tilde{x}(\tilde{z},\tilde{y}) = a_{max}e^{-\mu\tilde{z}}\sin\left(\frac{\omega}{v_T}\tilde{y}\right) \tag{26}$$

where $a_{\max}$ is maximum amplitude of the oscillation, measured at the base of the material, and μ is a decay constant.

We nondimensionalize Eq. 26 by the following:

$$\tilde{x} = a_{max}x, \quad \tilde{z} = Hz, \quad \tilde{y} = \frac{v_t}{\omega}y$$

Which yields the following:

$$x(z,y) = e^{-\beta z}\sin(y), \quad \beta = \mu H \tag{27}$$

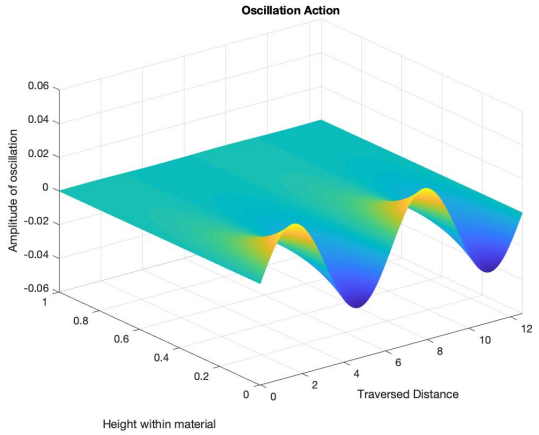

Figure 9: A plot of equation (27) which represents the material that has been eroded away by the oscillations.

4.1 Oscillation Magnification due to Erosion

We define orthogonal attack angle β as the deflection angle in the x direction and orthogonal displacement (x') relates to orthogonal attack angle as $\beta = \dfrac{\partial x}{dz}$.
To solve for the displacement orthogonal to the traverse, we calculate the change in orthogonal attack angle β (the angle of attack in the direction orthogonal to

the traverse) as proportional to the erosion rate for the side of the beam.

$$\frac{d\beta}{dz} = \frac{V^2}{\psi p K d(z)} f(\beta) \dot{M}_g \tag{28}$$

Numerically solving for β, we can then solve for the orthogonal displacement x' as a function of depth.

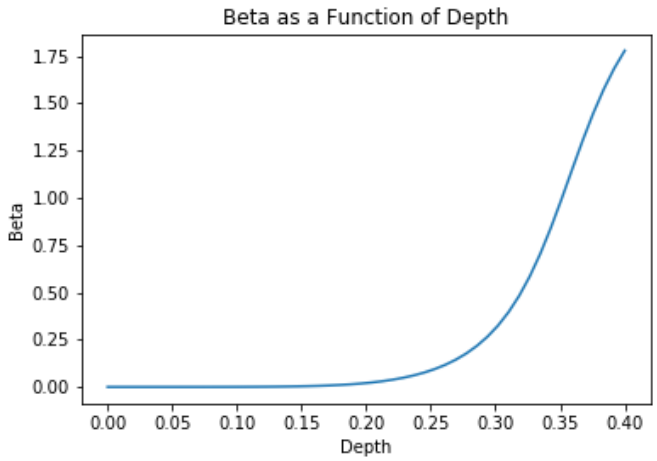

Figure 10: Orthogonal attack angle as a function of depth. Initial value of β is 10^{-6} radians.

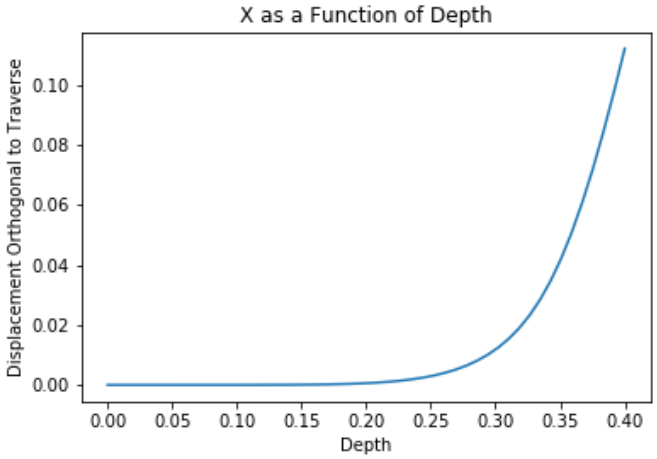

Figure 11: Displacement orthogonal to traverse as a function of depth.

Note that we observe a flat region where displacement is miniscule, followed by rapid growth. This agrees with experimental evidence, which shows smooth zones before striations begin.

Assuming an initial condition where the initial angle β has tiny periodic oscillations due to machine vibration, we then plot the exit displacement as a function of time.

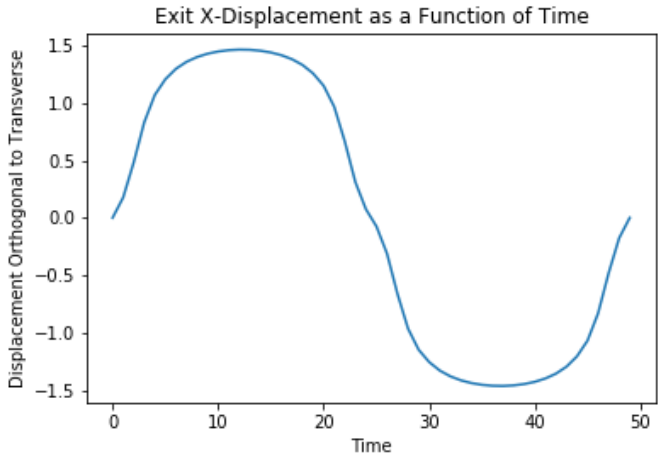

Figure 12: Displacement orthogonal to traverse at the exit as a function of time, assuming oscillating initial condition. Magnitude of initial angular displacement ranges between -10^{-6} radians and 10^{-6} radians

This model gives an explaination for the jet oscillations and why they seem to grow so quickly. Tiny perturbations to the jet when incident on the material, take some time to grow to be noticeable. However once they do so, they grow exponentially.

5 Conclusions

In considering the problems of striation formation and the curving of the striations, we assumed that these effects could be decoupled. As such we presented separate models for each.

We compared two models for the erosion from a waterjet on a slab of material. The Finnie model had the erosion directly proportional to the kinetic energy of the particles in the jet, while the Hashish model used a more complicated relation. Hashish also proposed a linear model for the velocity decay through the height of the material using conservation of momentum. This model for velocity was used in both the Hashish and Finnie models for erosion.

While the Hashish model was too numerically unstable to yield reliable results, the Finnie model demonstrated that the entirety of the material is eroded

during transit under the waterjet. Furthermore because the rate of erosion changes based on angle of attack and incident velocity, the erosion profile of the material was non linear which mimics the behavior seen in experiments.

To explain the side to side oscillations of the jet, we proposed a decaying sine function. We mapped this to data obtained from experiments to generate a mold of the oscillatory pattern of the jet.

For a more physical understanding, we considered the rate of change of the deflection angle in the x direction, β, with respect to depth to be dependent on the erosion rate at that depth as prescribed by the Finnie model. This differential equation was then solved, and the deflection was calculated as a function of β. This yielded results mirroring those seen in experiments.

These results may be validated with further experiments, yielding a physical explanation and model for the striation pattern formation. We feel these models were successful in explaining and illustrating these phenomena. For future work we may look at how these arguments may play into the kerf angle in the cut. We may also relax the assumption of jet uniformity, and take into account to runoff that is not immediately in the waterjet.

References

[1] F. L. Chen, J. Wang, E. Lemma, and E. Siores, *Striation formation mechanisms on the jet cutting surface*, Journal of Materials Processing Technology, 141 (2003), pp. 213–218.

[2] M. R. D. Arola, *Mechanism of material removal in abrasive waterjet machining of common aerospace materials*, in Seventh American Water Jet Conference, Seattle, 1993, pp. 43–64.

[3] I. Finnie, *Erosion of surfaces by solid particles*, wear, 3 (1960), pp. 87–103.

[4] Y. M. W. Y. F.L. Chen, E. Siores, *A study of surface striation formation mechanisms applied to abrasive waterjet process*, in CIRP International Symposium on Advanced Design and Manufacture in the Global Manufacturing Era, pp. 570–575.

[5] M. Hashish, *A modelling study of metal cutting with abrasive waterjets*, in J. Eng. Mater. Technol, 1984, p. 88–100.

[6] M. Hashish, *A model for abrasive waterjet machining*, Journal of Engineering Materials and Technology, 111 (1989).

[7] E. G. J. Chao, *Experimental study of the striation formation and spectral analysis of the abrasive water jet generated surfaces*, in Journal of Materials Processing Technology, 2003, pp. 213–218.

[8] M. R. S.P. Raju, *Predicting hydro-abrasive erosive wear during abrasive waterjet cutting*, in Manuf. Sci. Eng., ASME, 1994, p. 339–351.